PHYSICAL REVIEW D VOLUME 22, NUMBER 8 15 OCTOBER 1980

Quantum effects in the early Universe. IV. Nonlocal effects in particle production in anisotropic models

James B. Hartle
Department of Physics, University of California, Santa Barbara, California 93106
(Received 19 May 1980)

The dynamical equation governing the evolution of the effective geometry in the presence of the production of conformally invariant scalar particles is solved for a homogeneous model cosmology with small anisotropy and classical radiation. The pair-production probabilities and spectrum are calculated in the one-loop approximation to lowest nonvanishing order in the deviation from exact isotropy.

In this paper we shall continue the study begun in three earlier papers of a model calculation of particle production and anisotropy dissipation in the early Universe.[1-3] The model we consider is the production of free conformally invariant scalar particles in a slightly anisotropic, homogeneous, spatially flat model cosmology containing classical radiation. In previous papers we reduced the calculation of the particle-production probabilities in this model to the solution of a single linear integrodifferential equation. In paper III we were able to exhibit the qualitative behavior of solutions to this equation by solving it in a truncation in which nonlocal effects were neglected. In this paper we will complete the model by exhibiting solutions to the full integrodifferential equation and calculating the consequent pair-production probabilities.

The assumptions of the model, the effective-action equations used to compute the particle-production probabilities, and the approximations and truncations used to solve them are discussed in detail in the previous papers in this series. In summary, however, the basic points are the following: We compute the effective action $\Gamma[\tilde{g}]$ to first order in $\hbar$ for argument geometries $\tilde{g}$ of the homogeneous, spatially flat form

$$ds^2 = a^2[-d\eta^2 + (e^{2\beta})_{ij}dx^i dx^j], \tag{1}$$

where the scale factor a and the traceless 3×3 matrix β_{ij} describing the anisotropy are both functions of η alone. Only the contributions of a single conformally invariant scalar field are retained in the one-loop quantum corrections to the classical action. The result is calculated to quadratic order in the metric parameter β measuring the anisotropy,

$$\Gamma[a,\beta] = \Gamma_0[a] + \Gamma_2[a,\beta] + \cdots . \tag{2}$$

The dynamical equations

$$\delta\Gamma/\delta a = 0, \tag{3a}$$

$$\delta\Gamma/\delta\beta_{ij} = 0 \tag{3b}$$

determine a family of physically reasonable effective geometries[4] when subject to boundary conditions which exclude runaway expansions and fix the amount of anisotropy in the model. A convenient measure of this anisotropy is the parameter Δ defined in terms of the late time mean, H, and rms difference, ΔH, of the three principal Hubble constants by

$$\Delta^2 = \frac{1}{6}\left[\left(\frac{\Delta H}{H}\right)^2 \frac{1}{l^2\rho_r^{1/2}}\right]_{\eta=\infty}, \tag{4}$$

where ρ_r is the density of classical radiation and $l = (16\pi G)^{1/2}$ is the Planck length. Δ is dimensionless, scale invariant, and constant in classical epochs.

To quadratic order in the anisotropy of the model, the probability to produce a pair of scalar particles over the whole history of the Universe in a comoving spatial volume V is

$$P = \frac{V}{960\pi}\int d\eta\, \bar{\beta}''_{ij}\beta''^{ij}, \tag{5}$$

where a prime denotes a derivative with respect to η. In this expression β_{ij} is the solution to Eq. (3b), where Γ_2 has been evaluated at the solution a_0 of Eq. (3a) in the limit of exact isotropy.

In paper I we found the class of physically reasonable solutions to Eq. (3a) in the limit of exact isotropy. For one of these geometries the initial singularity occurred at $\eta = -\infty$ so that it was conformal to a complete flat spacetime and free from cosmological particle horizons. Further attention was focused on this case and this is the sole case considered here. In paper III the dynamical equation (3b) for β_{ij} was discussed. By introducing the constants $\tilde{\rho}_r = a^4\rho_r$, $\gamma = 6^{1/2}/\tilde{\rho}_r^{1/4}$, $\lambda = (2880\pi^2)^{-1}$, and scaled variables b, χ, and h through

$$a_0 = l\tilde{\rho}_r^{1/4} b, \tag{6a}$$

$$\eta = \gamma\chi, \tag{6b}$$

$$\beta'_{ij} = (\gamma^2/3\lambda)c_{ij}h, \tag{6c}$$

the dynamical equation can be written

$$\frac{d}{d\chi}\left(A\frac{dh}{d\chi}+K\frac{dh}{d\chi}\right)+Bh=1, \tag{7}$$

where

$$A=-\frac{i\pi}{2}-\ln(\mu_1 b) \tag{8}$$

and

$$B=\frac{2b^2}{\lambda}-\frac{1}{3}\left(\frac{b'}{b}\right)^2-\frac{1}{3}\left(\frac{b''}{b}\right). \tag{9}$$

The operator K is defined by

$$Kf(\chi)=Cf(\chi)-\tfrac{1}{2}\int_{-\infty}^{+\infty}d\chi'\,\epsilon(\chi-\chi')\ln|\chi-\chi'|\,\frac{df}{d\chi'}, \tag{10}$$

where C is Euler's constant and $\epsilon(\chi)=\chi/|\chi|$. In these relations the constant μ_1 is the unfixed regularization scale while c_{ij} is a measure of the magnitude and orientation of the overall anistropy related to Δ^2 by

$$\Delta^2=\gamma^6 c_{ij}c^{ij}/216. \tag{11}$$

The single function $h(\chi)$ thus controls how the anisotropic part of the effective goemetry varies with time while the constant Δ^2 measures the magnitude of the anisotropy in the model.

In paper III we showed that, if it existed, there was a unique solution to Eq. (7) for which the total pair-production probability given by Eq. (5) was finite. The appropriate boundary conditions for the conformally complete a_0 which yield this solution are

$$h(\chi)\sim\lambda/(2\chi^2),\quad \chi\to+\infty \tag{12a}$$

$$h(\chi)\sim-(3\lambda/8)^{1/2},\quad \chi\to-\infty. \tag{12b}$$

In paper III we exhibited solutions to Eq. (7) only in the local truncation in which the nonlocal integral $K(dh/d\chi)$ in Eq. (7) was neglected. The resulting ordinary differential equation could then be straightforwardly solved by shooting. There was, however, no justification for neglecting the nonlocal integral $K(dh/d\chi)$ in favor of the comparable term $A(dh/d\chi)$. In this paper we will exhibit solutions to the full integrodifferential equation (7).

Equation (7) was solved by converting it to a system of simultaneous linear equations for the values of $h(\chi)$ at a set of uniformly spaced points between a minimum value χ_0 and a maximum χ_1. The differential part was differenced by standard methods. The integral $(d/d\chi)[K(dh/d\chi)]$ has a logarithmically singular kernel and required some care. We first noted that with the boundary conditions of Eq. (12) $(d/d\chi)[K(dh/d\chi)]=K(d^2h/d\chi^2)$, so that from Eq. (10) the nonlocal term is the integral of the logarithmically singular kernel over $d^3h/d\chi^3$. The derivative $d^3h/d\chi^3$ was differenced by standard methods. The logarithmically singular integral $\int d\chi'\,\epsilon(\chi-\chi')\ln|\chi-\chi'|g(\chi')$ was treated by deriving an integration formula interpolating the argument $g(\chi)$ linearly between the mesh points but evaluating the logarithm exactly. Since $\int d\chi\ln\chi$ is well behaved at $\chi=0$ this gave a finite integration formula. The resulting set of linear equations on the equally spaced mesh between χ_0 and χ_1 was supplemented with the additional linear equations expressing the boundary conditions $h(\chi_0)=-(3\lambda/8)^{1/2}$ and $h(\chi_1)=0$. The whole system of equations was then solved using a complex matrix inversion routine. Reasonable results were obtained with a step size $\Delta\chi=0.0125$ and a range $\chi_0=-0.8$, $\chi_1=1.2$. Halving the step size changed the results by not more than about 5% pointwise. Extending the value of χ_1 to 1.6 or contracting the value of χ_0 to -0.4 did not change the results significantly, indicating that the values $\chi_0=-0.8$, $\chi_1=1.2$ are sufficiently far in the asymptotic regions that enforcing the boundary conditions mentioned above, at the finite points χ_0 and χ_1, are good approximations to the true asymptotic boundary conditions of Eq. (12).

The results of our calculation are shown in Figs. 1–6 for three different values of the unfixed regularization scale μ_1 measured in Planck units. Figure 1 shows the real part of h in the range

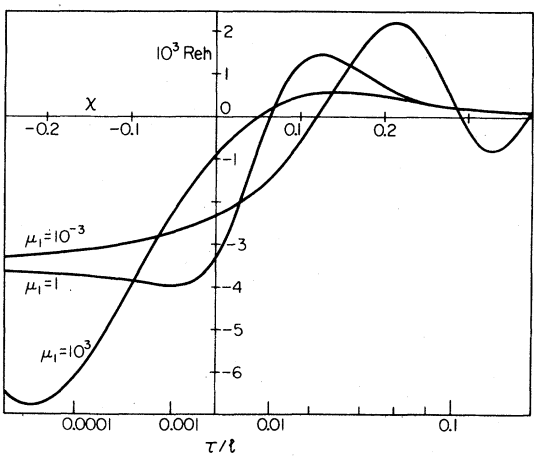

FIG. 1. The real part of the solution h of the dynamical equation which constrols the evolution of the anisotropic part of the effective geometry for three different values of the unfixed regularization scale μ_1. In all three cases the function h approaches the real constant $(3\lambda/8)^{1/2}$ at the singularity ($\chi\to-\infty$) and evolves classically as (real const)/χ^2 at late times ($\chi\to+\infty$). The bottom scale measures the proper time of a stationary observer from the singularity in units of the Planck time.

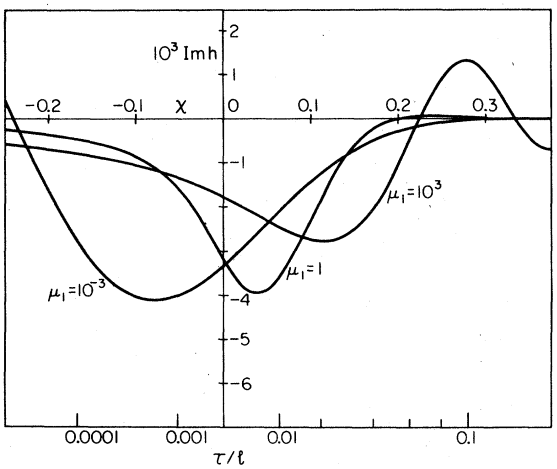

FIG. 2. The imaginary part of the function h on the same scales of Fig. 1. The imaginary part vanishes as $\chi \to +\infty$. For typical values of μ_1 shown here it is significant for τ less than a few tenths of the Planck time.

$-2.5 < \chi < 3.75$ or correspondingly in the range $\tau/l < 0.1$, where τ is the proper time from the singularity as measured by a comoving observer. Figure 2 shows the imaginary part of h. Although qualitatively similar in both form and magnitude, the details of the effective geometry are sensitive to the value of μ_1. For $\mu_1 = 1$ and 10^3, the geometry is essentially classical by $\tau \sim 0.1l$. The imaginary part is negligible after this time and the real part decays according to the classical law $h \sim \chi^{-2}$. For $\mu_1 = 10^{-3}$, this classical epoch sets in

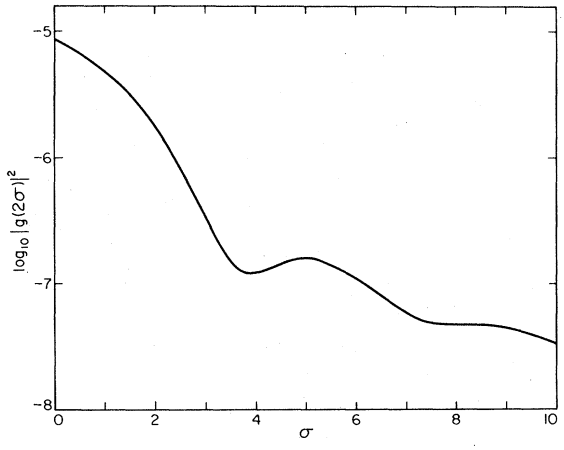

FIG. 3. The spectrum of produced pairs for $\mu_1 = 1$. The quantity $|g(2\sigma)|^2$ is proportional to the probability of producing a pair of particles each of which has a scaled frequency σ in the range σ to $\sigma + d\sigma$. The frequency range of our calculation of the spectrum is limited by the numerical accuracy of our solution for h and in this regime the result is not very sensitive to the value for μ_1.

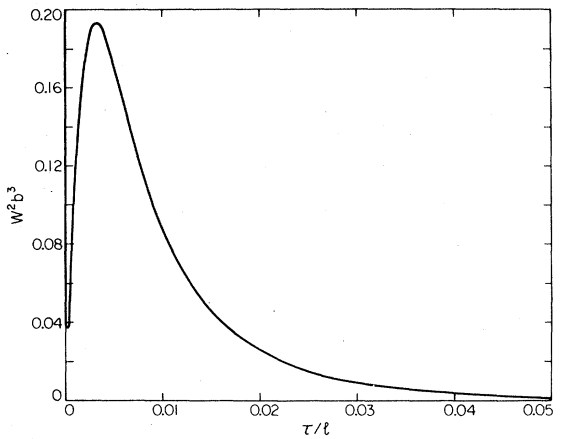

FIG. 4. A measure of the particle production rate. The integral of the function W^2b^3 with respect to τ is the proportional to the total probability of producing a particle pair over the whole history of the Universe in a given comoving volume. W^2b^3 itself is thus a crude measure of the production rate. It is shown here for $\mu_1 = 1$ the curves corresponding to $\mu_1 = 10^3$ and $\mu_1 = 10^{-3}$ not differing greatly from this. This measure of the production rate becomes infinite at the singularity but slowly enough so that its integral is finite. The significant times for particle production are between the singularity and a few hundredths of a Planck time.

at somewhat later times $\tau \sim 0.7l$. The significant regime for quantum dynamics, for the production of particle pairs, and for the dissipation of anisotropy thus occurs at $\tau \lesssim l$—a very early time.

It is worthwhile comparing these results for $h(\chi)$ with Figs. 1, 2, and 3 of paper III which result from neglecting the nonlocal integral in the dynamical equation. The main feature which emerges is that, while the local truncation differs

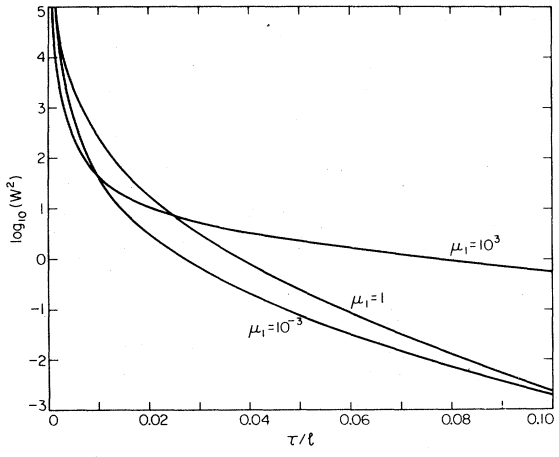

FIG. 5. The function W^2, which measures the absolute magnitude of the complex Weyl tensor of the effective geometry, plotted against proper time from the singularity for three values of the regularization scale μ_1.

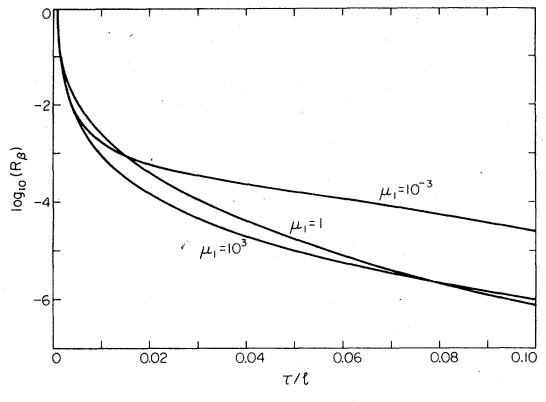

FIG. 6. The function R_β, which measures the magnitude of the anisotropy energy of the effective geometry, plotted against proper time from the singularity for three values of the regularization scale μ_1.

significantly from the full calculation pointwise, in qualitative form and order of magnitude it provides a good approximation to the behavior of the full solution. The chief effect of the nonlocal part of the equation is to concentrate the imaginary part of the result in a slightly narrower range of χ and to damp out some of the late time oscillations.

Having solved for the effective geometry we may now calculate the pair-production probability from the integral in Eq. (5) using the definitions in Eq. (6). The quantity with the most direct interpretation is the probability P_r to produce a pair of scalar particles over the whole history of the Universe in the comoving volume occupied by one of the classical radiation quanta. This is given in terms of h by Eq. (3.16) of paper III. Our main result is that this probability is finite. For the particular solutions calculated here we find

$$P_r=\begin{cases}6.1\times10^2\Delta^2, & \mu_1=10^{-3}\\ 5.8\times10^2\Delta^2, & \mu_1=1\\ 7.0\times10^2\Delta^2, & \mu_1=10^3\end{cases} \tag{13}$$

with an estimated accuracy of about 10%. These results for the pair-production probability are to be applied only for Δ^2 such that $P_r\ll1$, which gives a quantitative meaning to the approximation of small anisotropy. The results in Eq. (13) show that the pair-production probability is not very sensitive to the value of the unfixed regularization scale μ_1 and comparison with the result of the local calculation ($6.2\times10^2\Delta^2$ for $\mu_1=1$) shows that it is not much altered by the inclusion of nonlocal effects.

The spectrum of the produced particles may also be calculated from the effective geometry as discussed in Sec. IV of paper III. The probability density $p(\omega)$ of producing a pair each member of which has a frequency ω [in the sense that it corresponds to a solution of the scalar wave equation varying as $\exp(-i\omega\eta)$] is proportional to $|g(2\sigma)|^2$, where $g(\sigma)=\int d\chi\,\exp(i\sigma\chi)(dh/d\chi)$ and $\sigma=\gamma\omega$. A curve of $|g(2\sigma)|^2$ for $\mu_1=1$ is shown in Fig. 3 for the limited range of σ allowed by the accuracy of the numerical solution for h. Curves for $\mu_1=10^3$ or $\mu_1=10^{-3}$ differ very little from this one in this range of σ. The main conclusion to be drawn from this figure is that the spectrum does not vary exponentially with σ as in a thermal distribution but displays some structure.

The effective geometry by itself is not related in a precise way to the local rate of particle production. The total rate of particle production in Eq. (5), however, is expressed as an integral over time so that the argument may be viewed as a crude measure of this rate. If we write

$$P=\int_0^\infty d\tau\,p(\tau), \tag{14}$$

where τ is the proper time from the singularity then $p(\tau)$ is proportional to W^2b^3, the quantity W^2 being defined by

$$W^2=\frac{2}{b^4}\left|\frac{dh}{d\chi}\right|^2. \tag{15}$$

Figure 4 shows a graph of W^2b^3. This measure of the rate approaches infinity at the singularity but slowly enough that the integral for the total probability [Eq. (14)] converges. The major contribution to the total probability integral comes from the times before a few hundredths of a Planck time. A comparison with Fig. 6 of paper III shows that the effect of the inclusion of nonlocal effects is to push the domain of significant particle production to earlier times. The strong dip and peak evident in Fig. 4 is, to some extent, an artifact of our choice of time variable. The rate measured with the χ coordinate time, for example, displays a smooth single peak.

We turn now to the question of the dissipation of anisotropy in the model. A complete quantum mechanical description of the evolution would involve the construction of the amplitude to go from various initial anisotropic states to all possible final ones. This we have not done. We have, however, solved for the effective geometry—the suitably gauge-averaged normalized matrix element of the metric field between the initial and final vacuums. This, for example, would be one matrix element contributing to a calculation of the evolution of the expectation value of any measure of the anisotropy in the initial state. It is therefore appropriate to examine the local measures of the anisotropy in the effective geometry; Figs. 5 and 6 show two of them.

Figure 5 shows the quantity W^2 plotted against

proper time from the singularity. W^2 is related to the absolute square of the Weyl tensor by

$$\overline{C}_{\alpha\beta\gamma\delta}C^{\alpha\beta\gamma\delta}=4\Delta^2W^2/(\lambda^2t^4) \tag{16}$$

and is thus one measure of the anisotropy in the effective geometry. A second measure is Misner's anisotropy energy[5] ρ_β defined as the absolute square of the shear and given in the present notation for small anisotropies by $\overline{\beta}'_{ij}\beta'^{ij}/a^2$. Figure 6 shows the quantity $R_\beta=|h|^2/b^2$ which is related to the anisotropy energy by

$$\rho_\beta=4\Delta^2R_\beta/(\lambda^2t^4), \tag{17}$$

plotted against proper time from the singularity. Both W^2 and R_β are infinite at the singularity but decrease rapidly away from it. The decrease is slightly faster than that computed in the absence of nonlocal effects, as can be seen by a comparison with Figs. 4 and 5 of paper III. The decrease, however, is not strikingly different in form from that which would be predicted for these quantities by the classical laws. For example, in classical relativity the Weyl tensor decays as t^{-5} while the anisotropy energy decays as t^{-3}. These behaviors, normalized to agree with the quantum calculation for h at late times, are at early times quite close to those of the quantum calculation. This is plausibly a consequence of the restriction of the anisotropies in the model to be small with a consequent small effect on the dynamics.

Thanks are due B. L. Hu for many discussions and to S. Shapiro for a useful conversation on numerical methods. This work was supported in part by the National Science Foundation.

---

[1]M. V. Fischetti, J. B. Hartle, and B. L. Hu, Phys. Rev. D 20, 1757 (1979), paper I.

[2]J. B. Hartle and B. L. Hu, Phys. Rev. D 20, 1772 (1979), paper II.

[3]J. B. Hartle and B. L. Hu, Phys. Rev. D 21, 2756 (1980), paper III.

[4]We use the term "effective geometry" for the suitably gauge-averaged matrix element $\langle 0_+|g_{\alpha\beta}|0_-\rangle/\langle 0_+|0_-\rangle$ as less confusing than the term "classical geometry" of earlier papers.

[5]C. W. Misner, Astrophys. J. 151, 431 (1968).